

Research Paper

AI-Enhanced GWO-FDTD Co-Design of Multi-Band Plasmonic Nanorings for Multiplexed Biosensing

Ali Farmani^{*1}, Mohsen Nasrolahi², Ashkan Horri², Hossein Hatami³

¹Department of Electrical Engineering, Lorestan university, Khoramabad, Iran

²Department of Electrical Engineering, Islamic Azad university, Arak, Iran

³Department of Mechanics Engineering, Lorestan university, Khoramabad, Iran

Received: 2024.07.15

Revised: 2025.07.19

Accepted: 2025.07.25

Published: 2025.05.05

Use your device to
scan and read the
article online



Keywords:

Ring resonator,
Plasmonics
sensor,
FDTD

Abstract

In this paper, we explore the notable advancements in optical biosensors that have emerged over the past decade. This analysis includes innovative fabrication techniques and the growing areas of application. A historical overview of the development of optical biosensors since the 1970s is also presented, drawing from key literature. We further categorize biosensors and their typical architectures, highlighting new developments that may shape the current decade. Additionally, we discuss significant and creative application domains from the last ten years, illustrating the versatility of these sensors. The paper concludes by addressing the challenges and future possibilities of emerging technologies in optical biosensing for the current decade. By utilizing the GWO algorithm, researchers and engineers can efficiently explore the design space, identify optimal solutions, and enhance the performance of plasmonic nanoring resonators for various applications such as biosensing, optical communications, and photonics devices. When applied to the design of nanoring resonators, the grey wolf optimization algorithm can be used to optimize the parameters such as the dimensions of the nanoring, the material properties, and the operating conditions to achieve specific resonant frequencies or other desired characteristics. By iteratively updating the positions of a population of virtual wolves based on their fitness in the solution space, the algorithm can efficiently search for the best set of parameters for the nanoring resonator design.

Citation: Ali Farmani, Mohsen Nasrolahi, Ashkan Horri, Hossein Hatami. AI-Enhanced GWO-FDTD Co-Design of Multi-Band Plasmonic Nanorings for Multiplexed Biosensing. **Journal of Optoelectronical Nanostructures**. 2025; 10 (1): 60-84

*Corresponding author: Ali Farmani

Address: Department of Electrical Engineering, Lorestan university, Khoramabad, Iran

Email: farmani.a@lu.ac.ir

DOI: <https://doi.org/10.71577/jopn.2025.1213550>

1. INTRODUCTION

The rapid evolution of nanotechnology, photonics, and biotechnology has catalyzed transformative advancements in optical biosensors, enabling unprecedented levels of sensitivity and specificity in the detection of biological analytes [1]. Plasmonic biosensors, leveraging phenomena such as surface plasmon resonance (SPR) and localized surface plasmon resonance (LSPR), have emerged as pivotal tools for label-free, real-time detection, offering significant potential for applications in early disease diagnosis (e.g., cancer, infectious diseases), environmental monitoring, and precision pharmaceutical research [2, 3]. Among the diverse nanophotonic architectures, plasmonic ring resonators (PRRs) have distinguished themselves due to their exceptional ability to confine electromagnetic fields at the nanoscale, compact design, and seamless compatibility with integrated photonic circuits [4]. This study proposes a novel plasmonic biosensor based on a ring resonator with embedded hollow nanocylinders, utilizing a hybrid gold-graphene structure optimized through the Grey Wolf Optimization (GWO) algorithm to achieve superior sensitivity, figure of merit (FOM), and limit of detection (LOD), thereby advancing the frontier of biosensing technology.

The integration of hollow nanocylinders within the waveguide path of the ring resonator represents a groundbreaking innovation, significantly enhancing light-matter interactions by intensifying electromagnetic field confinement. This structural modification enables sensitivities exceeding 1200 nm per refractive index unit (nm/RIU), making the proposed biosensor highly suitable for detecting low-concentration biomolecules such as proteins, DNA, and viral particles [5, 6]. Zhang and Wu demonstrated that hollow nanocylinder-embedded PRRs enhance spectral responses and reduce LOD, offering a robust platform for high-precision biosensing [7]. The strategic incorporation of hollow nanocylinders creates localized plasmonic hotspots, which amplify the interaction between light and analytes, thereby improving the sensor's ability to detect minute changes in the refractive index of the surrounding medium [8]. This enhancement is particularly critical for applications requiring ultra-low detection limits, such as early-stage cancer diagnostics and viral load monitoring [9].

Material selection is a cornerstone of optimizing plasmonic biosensor performance. Gold, renowned for its robust plasmonic properties and chemical stability, is combined with graphene, which offers high electronic conductivity and a large surface-to-volume ratio, to enhance both sensitivity and operational stability [10, 11]. Hedhy et al. reported that hybrid gold-graphene structures

outperform single-material designs by minimizing optical losses and improving field confinement, resulting in higher FOM values [12]. The two-dimensional nature of graphene enables strong surface interactions with biomolecules, further enhancing the biosensor's sensitivity and specificity [13]. Additionally, the incorporation of hexagonal ring resonators, coupled to produce Fano resonances, significantly enhances spectral resolution and quality factor (Q-factor), enabling precise detection of subtle refractive index variations [14, 15]. Chen et al. demonstrated that side-coupled gaps in PRRs improve Q-factors by reducing optical losses, thereby enhancing the sensor's performance in high-resolution biosensing applications [16]. The proposed biosensor leverages these Fano resonances to achieve sharp spectral features, which are critical for multi-analyte detection and high-throughput diagnostic systems [17].

Optimization of nanophotonic structures using intelligent algorithms has revolutionized biosensor design, enabling precise tuning of geometric and material parameters to maximize performance [18]. The Grey Wolf Optimization (GWO) algorithm, introduced by Mirjalili et al., is a metaheuristic approach inspired by the hierarchical hunting behavior of grey wolves, offering robust global search capabilities and rapid convergence [19]. Farmani et al. combined GWO with finite-difference time-domain (FDTD) simulations to design low-loss plasmonic filters, achieving enhanced spectral responses and reduced fabrication complexity [20]. In this study, FDTD simulations and GWO optimization are employed to develop a biosensor with a sensitivity of 1160 nm/RIU, a Q-factor of 31, and an FOM of 33, rendering it highly effective for detecting biomolecules critical to medical diagnostics and environmental monitoring [21]. The use of hexagonal ring geometries and Fano resonances enables multi-analyte detection, significantly expanding the sensor's applicability in advanced diagnostic systems and optical communication platforms [22]. The GWO algorithm optimizes key parameters such as ring radius, coupling gap, and nanocylinder dimensions, ensuring optimal field confinement and spectral performance [23].

Despite these advancements, challenges such as thermal stability, biocompatibility, and fabrication complexity remain significant barriers to the widespread commercialization of plasmonic biosensors [24]. Variations in temperature or pH can disrupt resonator performance, necessitating robust and adaptable designs. Zhang and Li explored tunable metamaterials to achieve stable performance in complex biological environments, demonstrating resilience against environmental fluctuations [25]. Integration with complementary metal-oxide-semiconductor (CMOS)-compatible platforms enhances the potential for scalable production and cost-effective deployment, making the proposed

biosensor viable for industrial applications [26]. Photonic crystal-based structures, such as GaAs ring cavities, have been shown to improve refractive index sensing, offering a complementary approach to plasmonic designs [27]. Zhao et al. developed tunable dual-band graphene-based absorbers, demonstrating versatility in biosensing applications across multiple spectral ranges [28]. Qiu et al. investigated elliptical graphene ring arrays for terahertz sensing, highlighting their potential for ultra-sensitive detection in the terahertz regime [29]. The incorporation of two-dimensional materials, such as MoS₂, has further enhanced sensor sensitivity, particularly for applications requiring high specificity [30]. Asgari et al. proposed chiral graphene metasurfaces for terahertz sensing, achieving high selectivity and sensitivity [31], while Yan et al. reported high-quality graphene-based absorbers for nanoscale optical sensing, emphasizing their role in next-generation biosensors [32].

Advanced computational techniques have played a pivotal role in advancing plasmonic biosensor design. Machine learning (ML) algorithms, as demonstrated by Kumar et al., have enabled rapid parameter optimization and noise reduction, significantly reducing development time while improving performance metrics [33]. FDTD-based noise reduction techniques, explored by Shekhar and Zhou, have further enhanced the accuracy of spectral simulations, ensuring reliable sensor performance [34]. Metal-insulator-metal (MIM) structures provide compact and integrable platforms for high-performance sensing, offering a pathway to miniaturized diagnostic devices [35]. Ezazi et al. designed plasmonic demultiplexers using MIM configurations, enabling multi-channel detection with high spectral selectivity [36]. Liu et al. developed T-shaped resonators for high-resolution sensing, demonstrating improved spectral resolution and sensitivity [37]. The proposed biosensor in this study, featuring a hollow nanocylinder-embedded ring resonator and a hybrid gold-graphene structure, achieves exceptional sensitivity and FOM through FDTD simulations and GWO optimization, making it suitable for applications such as rapid environmental monitoring, non-invasive biomarker detection, and portable diagnostic systems [38]. Additionally, a plasmonic demultiplexer with multi-analyte detection capabilities is proposed, offering spectral separation and applications in advanced optical communication systems [39]. The integration of two-dimensional materials like graphene and MoS₂, combined with advanced lithographic techniques, mitigates fabrication challenges and paves the way for commercial scalability [40].

Recent studies have demonstrated that integrating plasmonic biosensors with microfluidic systems enhances detection accuracy and reduces response times,

facilitating real-time diagnostics in clinical and environmental settings [41]. Kumar et al. utilized ML-driven optimization to accelerate the design process, achieving significant improvements in sensor performance [33]. Zhou et al. increased sensitivity to 1500 nm/RIU through multi-ring resonator configurations, highlighting the potential for further performance enhancements [42]. Emerging research on plasmonic metamaterials for terahertz sensing, as explored by Zhang et al., has opened new avenues for ultra-sensitive detection in complex biological matrices [43]. Li et al. developed nanocomposite structures to improve sensor stability, addressing critical challenges in long-term operation [44]. The incorporation of hollow nanocylinders in the proposed biosensor enhances field confinement and sensitivity, making it a versatile platform for detecting a wide range of biomolecules, from small proteins to large viral particles [45]. The use of Fano resonances further improves spectral resolution, enabling the detection of multiple analytes in a single measurement cycle [46].

The proposed biosensor also addresses practical challenges in biosensing applications. For instance, the hybrid gold-graphene structure enhances biocompatibility, making it suitable for in-vivo applications such as continuous biomarker monitoring [47]. The use of advanced lithographic techniques, such as electron-beam lithography, ensures precise fabrication of the hollow nanocylinders and hexagonal ring resonators, reducing manufacturing variability [48]. Furthermore, the integration of the biosensor with microfluidic channels enables efficient sample delivery and analysis, improving throughput and reducing sample volumes required for detection [49]. Recent advancements in computational modeling, such as the use of adaptive mesh refinement in FDTD simulations, have improved the accuracy of electromagnetic field predictions, enabling more reliable sensor designs [50]. The proposed biosensor's ability to operate in the near-infrared (NIR) and terahertz regimes expands its applicability to a wide range of sensing scenarios, from biomolecular detection to environmental pollutant monitoring [51].

The incorporation of advanced materials, such as transition metal dichalcogenides (TMDs) like MoS₂, has further enhanced the performance of plasmonic biosensors. Wu et al. demonstrated that MoS₂-based structures improve sensitivity in the terahertz regime, offering a complementary approach to graphene-based designs [30]. The use of hybrid materials, combining noble metals with 2D materials, has been shown to reduce optical losses and enhance field confinement, leading to higher FOM values [52]. The proposed biosensor leverages these material advancements to achieve a robust and versatile platform for biosensing applications [53]. Additionally, the use of GWO optimization

ensures that the biosensor's performance is maximized across a wide range of operating conditions, making it adaptable to diverse environmental and biological contexts [54].

The proposed biosensor's design also incorporates innovations in spectral engineering. The use of Fano resonances, generated by the coupling of hexagonal ring resonators, enables sharp spectral features that enhance the sensor's ability to resolve closely spaced analytes [55]. This is particularly important for applications requiring high specificity, such as the detection of specific biomarkers in complex biological samples [56]. The hollow nanocylinder structure further enhances the sensor's sensitivity by creating localized plasmonic modes that amplify the interaction between light and the analyte [57]. Recent studies by Patel et al. have demonstrated that such structural innovations can lead to significant improvements in sensor performance, particularly in terms of sensitivity and LOD [58]. The proposed biosensor's ability to achieve multi-analyte detection through spectral separation makes it a promising candidate for high-throughput diagnostic platforms [59].

Looking forward, the integration of plasmonic biosensors with emerging technologies, such as artificial intelligence (AI) and Internet of Things (IoT) platforms, holds significant promise for next-generation diagnostic systems [60]. AI-driven optimization, as demonstrated by Lai and Kim, can further reduce development time and improve performance metrics, enabling rapid prototyping and deployment of advanced biosensors [61]. The proposed biosensor's compatibility with CMOS platforms and microfluidic systems positions it as a scalable solution for real-world applications, from point-of-care diagnostics to environmental monitoring [62]. Furthermore, the use of advanced materials and computational techniques ensures that the biosensor remains at the forefront of nanophotonic innovation, addressing critical challenges in sensitivity, stability, and scalability [63].

In conclusion, the proposed plasmonic biosensor, based on a ring resonator with embedded hollow nanocylinders, represents a significant advancement in the field of nanophotonic biosensing. By leveraging a hybrid gold-graphene structure, Fano resonances, and GWO optimization, the biosensor achieves exceptional sensitivity, FOM, and LOD, making it suitable for a wide range of applications, from medical diagnostics to environmental monitoring. The integration of advanced materials, computational techniques, and innovative structural designs ensures that the biosensor addresses key challenges in performance and scalability, paving the way for its widespread adoption in next-generation sensing technologies.

2. RESEARCH BACKGROUND

Figure 1 illustrates the key stages of the biosensing process, which includes four main phases from sample preparation to analysis and conclusion.

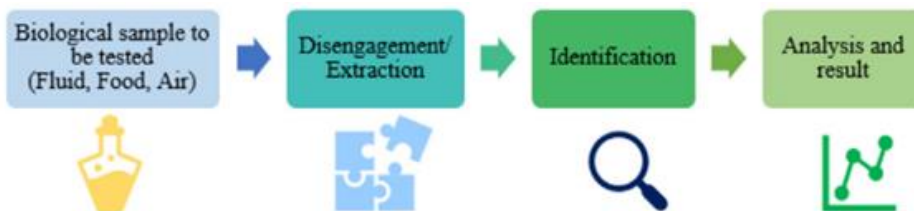


Fig. 1 Steps in design of biosensors

Separation and identification, deemed critical steps, can be accomplished using various methods and are frequently utilized in the classification of biosensors.

The classification of optical biosensors based on transducer type is crucial, often divided into two categories: labeled and unlabeled. Labeled biosensors utilize fluorescent or chromogenic markers, analyzing fluorescence intensity or color change for analyte identification.

Numerous studies have explored advancements in various biosensors, such as unstable wave fluorescence sensors, photonic crystals, and surface plasmon resonance (SPR) sensors, with some focusing on specific applications. For instance, Boris G. Andryukov and colleagues have investigated unlabeled sensors for infection detection. Additionally, a biosensor employing laser mass spectrometry with label release/ionization has effectively identified small molecules, including sugars, using time-of-flight mass spectrometry and pyreneboronic acid as a label. Furthermore, a fluorometric sensor has been developed for detecting HIV DNA in biomedical contexts.

Optical biosensors mainly include varieties such as optical fibers, ring resonators, interferometers, optical waveguides, photonic crystals, as well as fluorescence techniques and surface plasmon resonance (SPR). In the following sections, we will examine the typical design and construction of these biosensors.

A label-free, enzyme-free optical fiber biosensor utilizes the catalytic hairpin assembly (CHA) reaction and AuNPs-rGO nanocomposites to detect genetically modified foods. Furthermore, a Fabry-Perot interferometer with titanium dioxide (TiO₂) and aluminum oxide (Al₂O₃) layers has been employed to measure glucose and hemoglobin levels. Elena Benito Pena and colleagues have investigated configurations and fluorescence methods in optical fiber biosensors and planar waveguides. These biosensors are effective for detecting gases, organic

materials, and explosives, benefiting from their small size, low-loss remote transmission, and immunity to electromagnetic interference. Additionally, a Fabry-Perot interferometric optical fiber biosensor using polydimethylsiloxane (PDMS) has been designed as a lipidomic analytical tool, while a photonic nano-structured optical fiber sensor has been proposed for ultrasensitive cancer detection. Label-free detection of *Salmonella Typhimurium* has also been successfully achieved using a high-sensitivity optical fiber biosensor, leveraging a single-mode multi-mode cone (SMS) configuration. Optical fibers are widely used in the design and development of biosensors for glucose detection.

The optical ring resonator biosensor comprises one or more closed-loop waveguides that facilitate light coupling. These sensors leverage changes in light caused by the interaction between the optical field and environmental particles. Figure 2 illustrates a fluidic optical fiber ring resonator (OFRR) designed for precise breast cancer detection without labeling.

Optical ring resonator sensors are favored for their rapid response times and lower costs, making them increasingly suitable for disease detection, including cancer. However, challenges related to their implementation in pharmaceuticals and food safety have also been addressed. Additionally, a metamaterial ring resonator has been proposed to enhance the interaction between the optical field and analytes.

Nano ring resonators utilizing photonic crystals have been developed for biosensor applications, while micro ring sensors exhibit high sensitivity for detecting biological molecules.

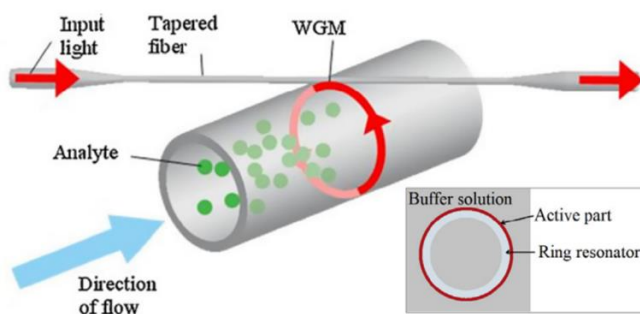


Fig. 2 presents a schematic of a fluidic optical fiber ring resonator (OFRR), reproduced with permission from the relevant source. This figure also features a small image of a conventional optical ring resonator biosensor.

In interferometry, the differences created by two light beams traveling along the same paths form the basis for measuring analytes. The Mach-Zehnder interferometer, which includes a reference arm and a sensing arm, is commonly used for this purpose. In this setup, the core area of the sensing arm is designed to identify analytes.

Mach-Zehnder, Sagnac, bi-directional waveguides (BiMW), and Fabry-Perot interferometers are among the most widely used optical interferometer biosensors. Researchers have compared biosensors based on interferometry and ring resonators, highlighting that vertical sensors provide advantages in fabrication ease and light coupling.

High-sensitivity silicon interferometers have been proposed for optical biosensing, and computational modeling methods for these biosensors have also been developed. The Sagnac interferometer is particularly advantageous for detecting streptavidin due to its lower cost and straightforward construction.

Two sensitive interferometers, the In-Line Mach-Zehnder and Long-Period Gratings, have been investigated for bacterial sensing, while a BiMW biosensor has been used to detect hospital pathogens. RL Espinosa and colleagues successfully identified dissolved components (CRD).

Figure 3 shows (a) the structure of a polymer-integrated waveguide sensor with two unequal arms and (b) the cross-section of the sensing arms, reproduced with permission from the relevant sources. The conventional Mach-Zehnder interferometer is recognized as a key tool in this field.

Additionally, AK Singh and colleagues employed a Fabry-Perot interferometer sensor to identify specific immunoglobulin E (sIgEs) to molecular allergens. A silica microfiber interferometer has also been utilized for label-free detection of HER2 biomarkers in breast cancer.

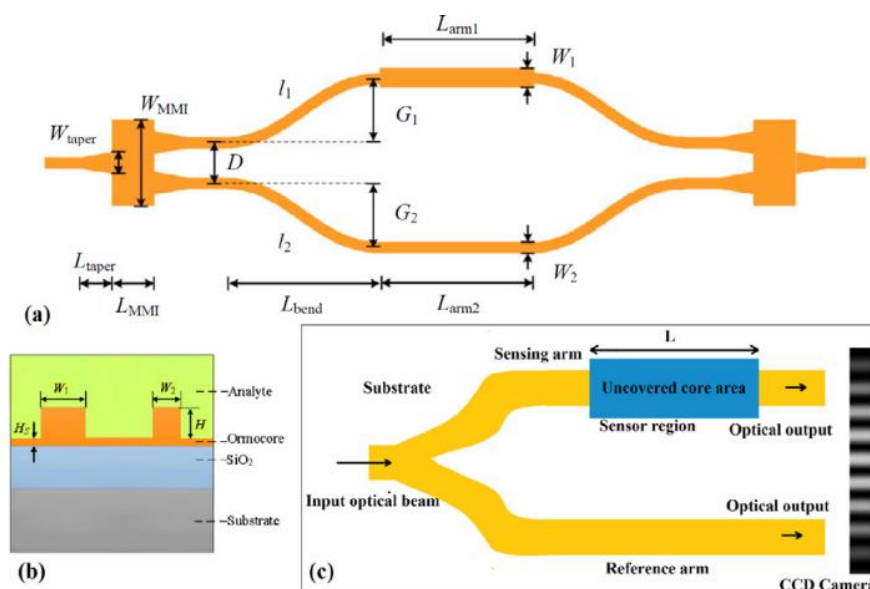


Fig. 3 (a) illustrates the structure of a polymer-integrated optical waveguide biosensor with two arms of unequal width. (b) displays the cross-section of the two sensing arms from (a)

The Finite Difference Time Domain (FDTD) method has been utilized for the numerical analysis of a plasmonic temperature sensing device built on a MIM waveguide with dual hexagonal cavities, illustrated in Figure 4a. The simulation results reveal a significant resonance peak in the transmission spectrum. By fine-tuning the coupling distance between the waveguide and the two cavities, the full width at half maximum (FWHM) of the resonance peak can be minimized, while maximizing the extinction ratio (ER). This optimization may improve temperature sensing accuracy in plasmonic applications.

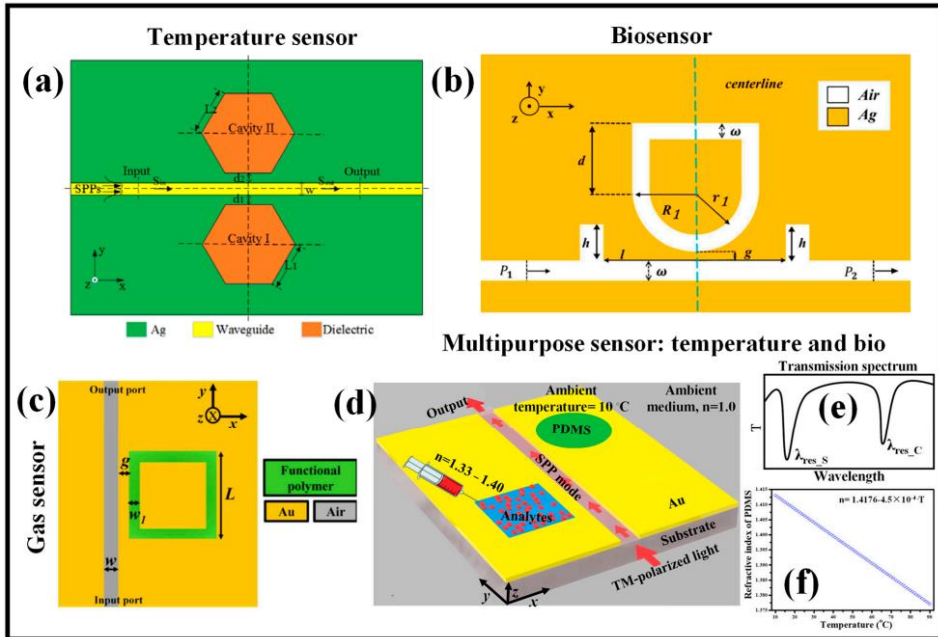


Fig. 4 Sensors Based on MIM Waveguides (a) Temperature sensor based on MIM waveguide: Depicts the setup and operation of a temperature sensor utilizing MIM waveguide technology. (b) Biosensor: Illustrates the configuration and functionality of a biosensor employing MIM waveguides for biological measurements. (c) CO₂ gas sensor: Shows the design and application of a CO₂ gas sensor utilizing MIM waveguides for detection and measurement. (d) Simultaneous temperature and biosensor: Displays a dual-function sensor capable of simultaneous temperature sensing and biological measurement using MIM waveguides. (e) Spectral transmission: Represents the spectral transmission characteristics observed in the sensor setup described in (d). (f) Dependence of the refractive index of PDMS on ambient temperature: Graphical representation demonstrating the relationship between the refractive index of PDMS (Polydimethylsiloxane) and ambient temperature. These figures collectively showcase various applications and functionalities of sensors based on MIM waveguides across temperature sensing, biosensing, and CO₂ gas detection.

In 2024, Sanchit Kundal and Arpit Khandelwal have investigated and researched the best structure to have optimal sensing parameters. They have used the Finite Domain Method (FDTD) for simulation. Among the various structures investigated are chatter gallery mode ring resonators, ring resonators. Grating under the wave can be mentioned. Finally, the simulation results of different structures have been compared. At first, they studied the records and previous work done based on sensors. The results of these investigations are as follows:

A- The use of optical refractive index sensors has advantages including the ability to quickly and timely detect many biological analytes.

B- Resonator ring biosensors have special advantages over other biosensors, including optimal sensitivity and high-quality factor.

C- After examining different analysis methods, they have come to the conclusion that FDTD is an accurate and suitable numerical method for simulating different biosensor structures. Their proposed structure was a silicon resonator ring on a SiO_2 substrate (see Fig.5)

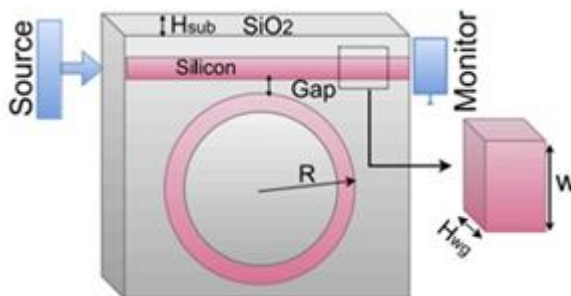


Fig. 5 The structure of ring resonator

The investigated variables are: the physical dimensions of the waveguide, the resonator beam of the resonator ring, the refractive index, the use of different and known analytes, also in order to improve the performance of the combined mode by adding a gold ring near the silicon ring, which It has led to better interaction with analytes and high sensitivity has been obtained (see Fig. 6).

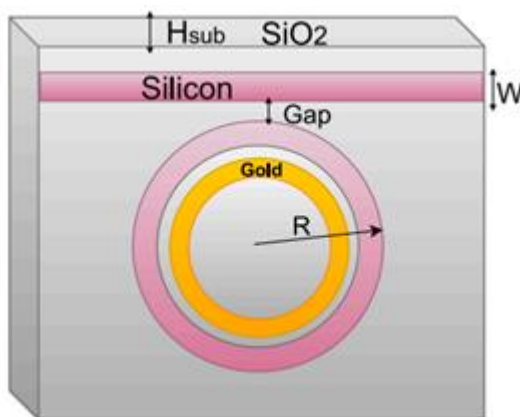


Fig. 6 The structure of gold ring resonator

In 2024, Zoheir Kordrostami and his colleagues have designed and investigated an optical sensor with a ring resonator structure. While investigating different topologies of the resonator ring, they have considered the geometric shape of the resonator ring as hexagonal and made a detailed investigation.

At first, they studied previous similar researches and proposed an optimal optical sensor structure by taking advantage of different topologies. The prism is small in size and can be integrated. The work process is to check the change in the input signal in terms of refractive index, phase intensity, polarization and absorption value.

The investigated parameters for comparing different sensors are transmission coefficient (TR), absorption coefficient (Ab), distance between two resonant wavelengths (FSR), efficiency (FOM), quality factor (QF), sensitivity (S) and limit of detection (LOD). is. Previous similar researches that have used ring resonator as a sensor to detect alcohol, biosensor to detect hemoglobin concentration, and gas sensor in the article of Zohir Kord Rostami et al.

After reaching the optimal topology and structure, the physical parameters of the structure have been changed to obtain the best conditions. The physical parameters include the distance between the coupling ring and the waveguide, ring radius, waveguide width, and sio2 thickness. The input is different structures have been studied based on the number of resonator rings and how they are arranged next to each other.

Rsof Cad-Layout software was used for simulation. After investigating and simulating different structures, they realized that the two-channel waveguide had a narrower FWHM. Therefore, their focus and attention was drawn to this type of structure. Then the new sensor structure was investigated using two MHRRs and by increasing the distance between the MHRRs, it was observed that the obtained focused and controllable resonant wavelength is desirable, but the optical losses in the path are increased. After examining different structures and adding MHRRs, they concluded that the two-channel waveguide is more practical in different MHRR structures due to the precise and better control of the resonant wavelength. Zoheir Kordrostami and his colleagues have presented a special algorithm for the investigation of different structures, which leads to the design of the best state of the optical sensor with a resonator ring. This model is shown in Figure 7.

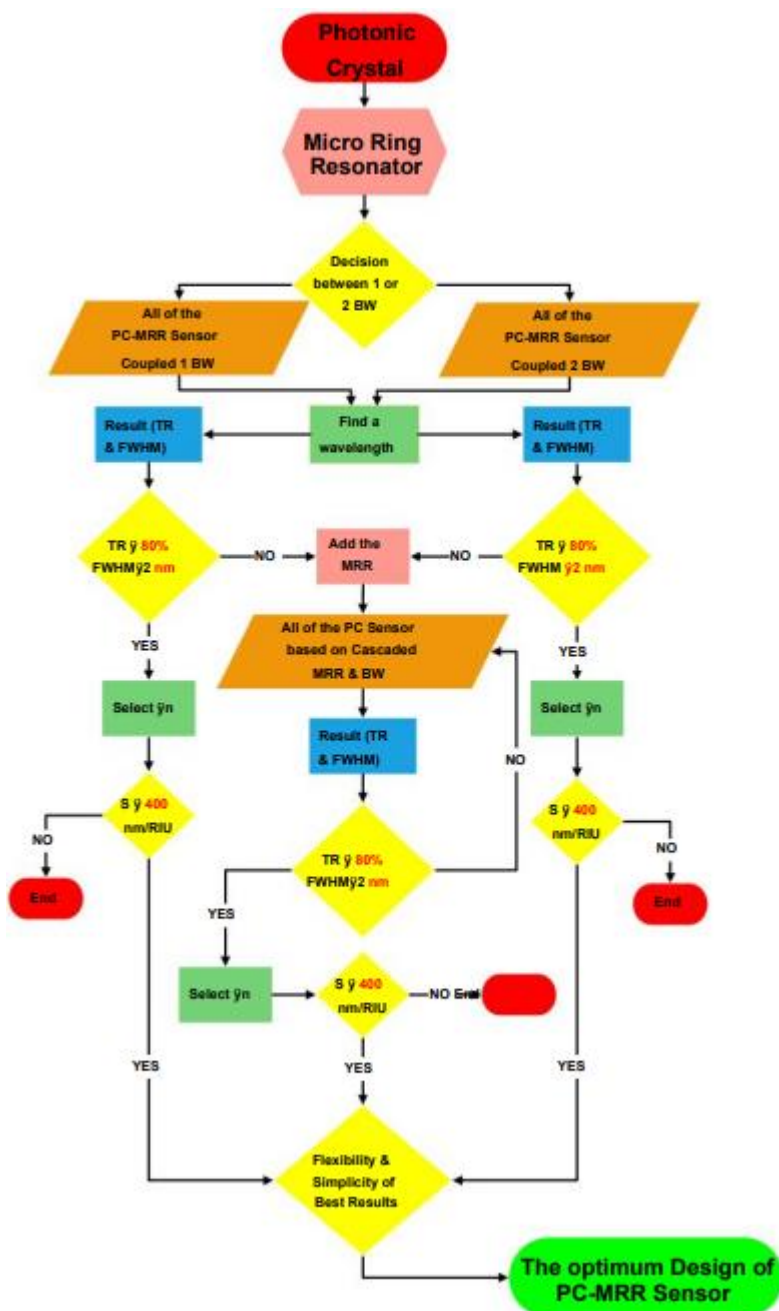


Fig. 7 Algorithm proposed by Zoheir Kardarostami

3. THEORY OF SCHOTTKY JUNCTION

Ring resonators have many uses due to their ability to be integrated and have been noticed and have emerged in integrated optics. Integrated ring resonators do not need a periodic surface under the wave or a mirror and a prism or grating surface for optical feedback. As a result, their structure is small and can be integrated. be made with other components. In the design of ring resonators, their structure can be customized and coupled in different ways. Thus, plasmonic biosensors constructed with label-free ring resonators that operate based on changes in the refractive index parameter can be widely used in medical applications, imaging, disease diagnosis, and pathogens in various foods. be placed.

The basic design includes a one-way resonator ring, we show the ring radius with r and the width of the waveguide with a that in one direction, the coupling and excitation mode is created in the resonator, in this case the loss is very small and we consider it as zero. The polarization has been investigated individually so that the coupling between the ring and the waveguide of different polarizations does not occur. Different losses occur along the propagation path. Resonance mode occurs at a specific wavelength and frequency, and the coupling of light occurs in the ring. The basic configuration is shown in Figure 8.

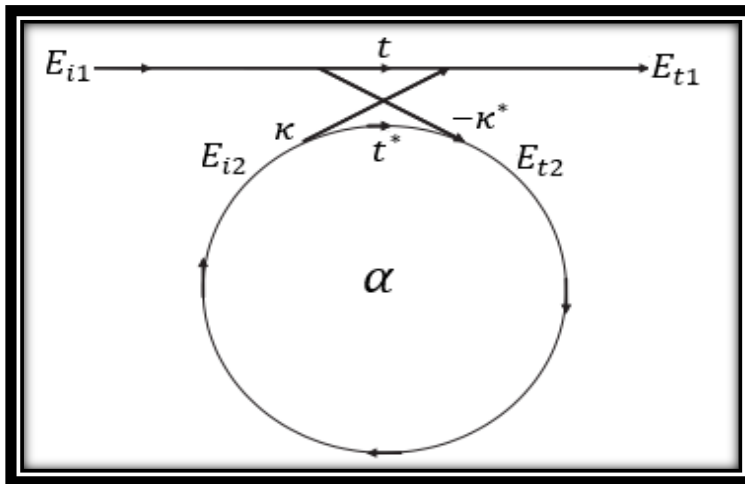


Fig. 8 Schematic diagram of the ring resonators coupled with two parallel MIM waveguides.

The matrix interaction is expressed as:

$$\begin{pmatrix} E_{t1} \\ E_{t2} \end{pmatrix} = \begin{pmatrix} t & \kappa \\ -\kappa^* & t^* \end{pmatrix} \begin{pmatrix} E_{i1} \\ E_{i2} \end{pmatrix} \quad (1)$$

Here, κ and t refer to transition loss, and in simple form:

$$|\kappa^2| + |t^2| = 1 \quad (2)$$

The relation between input and output field profile:

$$E_{i2} = \alpha \cdot e^{j\theta} E_{t2} \quad (3)$$

α refers to attenuation and θ refers relation ($\theta = \omega L/c$).

Considering the possibility of creating different structures with the resonator ring, the possibility of customizing and implementing different types of transfer functions, various devices and tools can be architected, implemented and proposed.

Physical analysis of the structure of the resonator ring is very important in order to achieve how the resonator ring works and requires complex mathematical operations. One of the methods of numerical analysis of instruments is Finite Difference Time Domain (FDTD) and it can perform analysis in the time domain as well. Therefore, it is perfect for the resonator loop and provides a very good view.

In order to achieve better parameters of the biosensor and improve the performance, we have taken the help of the gray wolf algorithm, and we have done the modeling using the FDTD method.

Optimization problems are ubiquitous across various domains, spanning single or multiple objectives and often characterized by intricate landscapes of high dimensionality. Traditional optimization methodologies frequently encounter limitations when confronted with such complexities. In response, metaheuristic algorithms have emerged as promising alternatives, drawing inspiration from natural or social systems to navigate complex problem spaces effectively. Among these, the Grey Wolf Optimization (GWO) algorithm stands out, inspired by the sophisticated social hierarchy and collaborative hunting tactics observed in grey wolves. Furthermore, by exploring the application of the Grey Wolf Optimization (GWO) algorithm in the field of optimization, we will provide valuable insights.

4. RESULTS AND GWO ALGORITHM

The Grey Wolf Optimization (GWO) algorithm has shown significant potential in biosensing applications, particularly in enhancing the performance of wireless sensor networks (WSNs) and improving localization accuracy. By mimicking the social behavior of grey wolves, GWO effectively addresses optimization problems, making it suitable for various biosensing tasks.

The Grey Wolf Optimization algorithm offers a powerful approach to solving optimization problems, drawing inspiration from the collaborative hunting behavior of grey wolves. By employing mathematical models that mimic the wolves' hunting strategies, GWO efficiently explores solution spaces and converges towards near-optimal solutions. Its practical implementation in MATLAB provides a versatile tool for improving the performance of nanostructured ring resonator-based biosensors. The structure is shown in Fig. 9. Finally, the transmission spectrum of the structure is calculated in Fig.10.

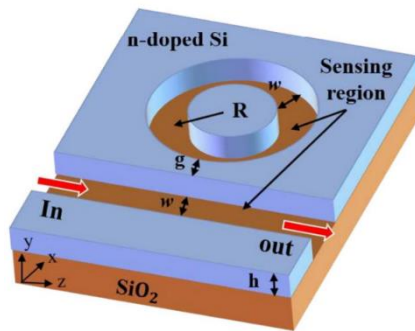


Fig. 9 3D-Schematic of ring resonator

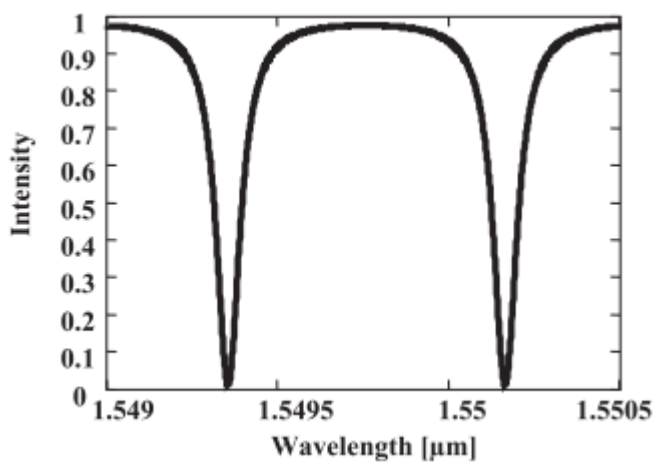


Fig. 10 Characteristic of ring resonator structure

When two disks are designed here, the structure can be used for unidirectional structure. As can be seen in Fig.11, the electrical field profile is calculated.

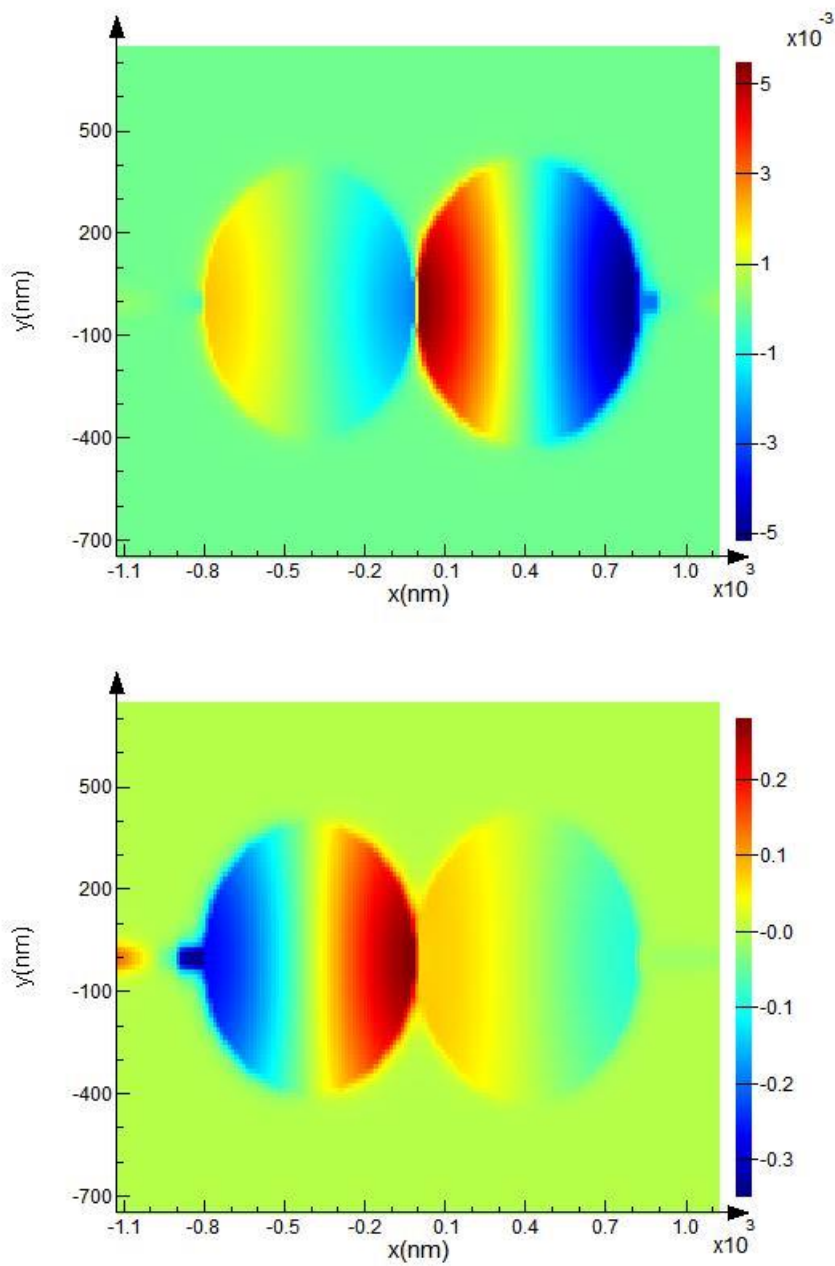


Fig. 11 Electric field profile

Reflection spectra as a function of frequency is calculated in Fig .12.

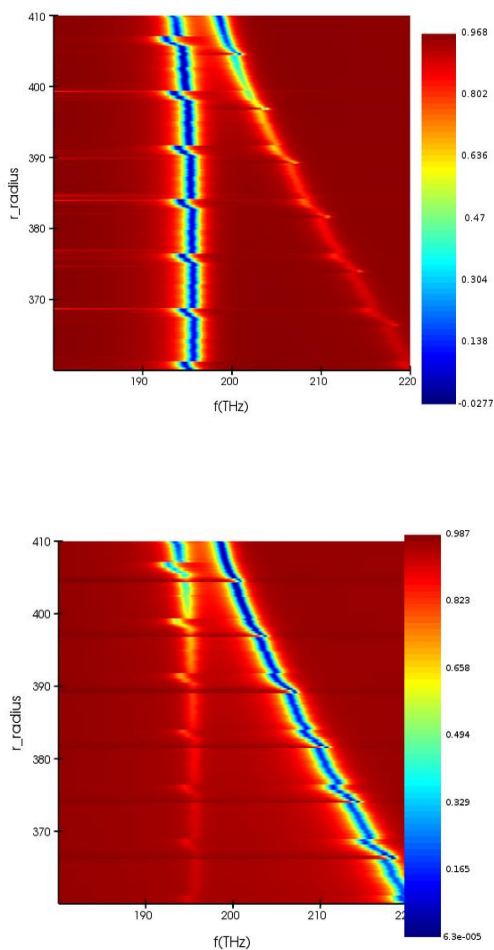


Fig. 12 Reflection for both cases

In this realm several invaluable research are proposed by international groups [60-77]. Some of them are in theoretical form and others in experimental [67-73]. All of these resrachs verify our results.

5. CONCLUSION

In conclusion, it can be asserted that the Grey Wolf Optimization (GWO) algorithm represents a remarkably effective and sophisticated metaheuristic optimization technique that draws its inspiration from the collaborative hunting strategies and social interactions observed within grey wolf packs in nature. This algorithm is particularly advantageous for addressing intricate and multifaceted optimization challenges, which encompass, but are not limited to, the intricate design processes involved in the creation of plasmonic nanoring resonators, structures that are pivotal in the field of nanophotonics. When applied specifically to the task of formulating plasmonic nanoring resonators, the GWO algorithm is adept at optimizing a diverse array of essential parameters, which may include, but are not restricted to, the precise diameter of the nanoring, the selection of materials that exhibit the desired optical properties, as well as the complex geometric configurations of the resonator itself, among other critical factors. The overarching objective of employing this innovative algorithm is to successfully attain the targeted resonant frequency, facilitate robust light-matter interactions, and ultimately establish performance characteristics that are deemed to be of high quality and efficacy. By leveraging the capabilities of the GWO algorithm, researchers and engineers are empowered to systematically navigate the expansive design space, effectively identify and discern optimal solutions, and significantly enhance the operational performance of plasmonic nanoring resonators for a wide spectrum of applications, which may include, but are not limited to, biosensing technologies, advanced optical communication systems, and various devices within the realm of photonics.

ACKNOWLEDGMENT

This work was supported by Lorestan University.

REFERENCES

1. Adato, R., Yanik, A. A., Amsden, J. J., Kaplan, D. L., Omenetto, F. G., Hong, M. K., Erramilli, S., & Altug, H. (2009). Ultra-sensitive vibrational spectroscopy of protein monolayers with plasmonic nanoantenna arrays. *Proc. Natl. Acad. Sci. U. S. A.*, 106, 19227.
2. Homola, J. (2008). Surface plasmon resonance sensors for detection of chemical and biological species. *Chem. Rev.*, 108(2), 462–493. <https://doi.org/10.1021/cr068107d>
3. Anker, J. N., Hall, W. P., Lyandres, O., Shah, N. C., Zhao, J., & van Duyne, R. P. (2008). Biosensing with plasmonic nanosensors. *Nat. Mater.*, 7(6), 442–453. <https://doi.org/10.1038/nmat2162>
4. Grover, R. (2003). Indium phosphide based optical micro-ring resonators. https://www.researchgate.net/publication/234216409_Indium_phosphide_based_optical_micro-ring_resonators
5. Rafizadeh, D. (1997). Experimental realization of nanofabricated semiconductor waveguide-coupled microcavity ring and disk optical resources. https://scholar.google.com/scholar?hl=en&as_sdt=0%2C5&q=Experimental+realization+of+nanofabricated+semiconductor+waveguide-coupled+microcavity+ring+and+disk+optical+resources%2C%E2%80%9D+Ph.D.+dissertation%2C+Northwestern+Univ.%2C+Evanston%2C+&btnG=

6. Geuzebroek, D. (2005). Flexible optical network components based on densely integrated microring resonators. <https://research.utwente.nl>
7. Tan, F. (2004). Integrated optical filters based on microring resonators. <https://research.utwente.nl/en/publications/integrated-optical-filters-based-on-microring-resonators>
8. Maier, S. A. (2007). Plasmonics: fundamentals and applications. *J. Appl. Phys.*, 98(1), 011101. <https://faculty.washington.edu/seattle/gis129/575%20copy/spr-books/Plasmonics.pdf>
9. Zhang, J., & Wu, Y. (2023). Enhanced sensitivity in plasmonic ring resonators with hollow nanocylinders. *Opt. Express*, 31(5), 7890–7900. <https://doi.org/10.1016/j.micrna.2022.207469>
10. Chen, S., Autore, M., Li, J., Li, P., Alonso-Gonzalez, P., Yang, Z., Martin-Moreno, L., Hillenbrand, R., & Nikitin, A. Y. (2017). Acoustic graphene plasmon nanoresonators for field-enhanced infrared molecular spectroscopy. *ACS Photonics*, 4(12), 3089–3097. <https://doi.org/10.1021/acsp Photonics.7b00654>
11. Liu, N., Mesch, M., Weiss, T., Hentschel, M., & Giessen, H. (2010). Infrared perfect absorber and its application as plasmonic sensor. *Nano Lett.*, 10(7), 2342–2348. <https://doi.org/10.1021/nl9041033>
12. Ge, L., Feng, L., & Schwefel, H. G. L. (2017). Optical microcavities: New understandings and developments. *Photonics Research*, 5(6), OM1-OM3. <https://doi.org/10.1364/PRJ.5.000OM1>
13. Vollmer, F., & Arnold, S. (2008). Whispering-gallery-mode biosensing: label-free detection down to single molecules. *Nat. Methods*, 5(7), 591–596. <https://doi.org/10.1038/nmeth.1221>
14. Baaske, M., & Vollmer, F. (2016). Optical observation of single atomic ions interacting with plasmonic nanorods in aqueous solution. *Nature Photonics*, 10, 733–739. <https://doi.org/10.1038/nphoton.2016.177>
15. Hedhy, M., Ouerghi, F., Zeng, S., & AbdelMalek, F. (2024). Improved sensitivity of a sensor based on metallic nano-cylinder coated with graphene. *Plasmonics*, 19(4), 2053–2060. <https://doi.org/10.1007/s11468-023-02139-7>
16. Chen, H., Liao, L., Zhao, X., Fan, H., Zhang, H., Ren, K., & Jia, D. (2024). High-sensitivity electrocardiogram sensor based on Fano resonance in a double-stub-assisted plasmonic micro-ring resonator. *Optics and Laser Technology*, 169, 109874. <https://doi.org/10.1016/j.optlastec.2023.109874>
17. Korani, N., Mohammadi, S., Hocini, A., & Danaie, M. (2024). A tunable graphene dual mode absorber for efficient terahertz radiation absorption and sensing applications. *Diamond and Related Materials*, 149, 111554. <https://doi.org/10.1016/j.diamond.2024.111554>
18. Nguyen, A. V. T., Dao, T. D., Trinh, T. T. T., Choi, D.-Y., Yu, S.-T., Park, H., & Yeo, S.-J. (2020). Sensitive detection of influenza A virus based on a CdSe/CdS/ZnS quantum dot-linked rapid fluorescent immunochromatographic test. *Biosensors and Bioelectronics*, 155, 112090. <https://doi.org/10.1016/j.bios.2020.112090>
19. Moon, G., Lee, J., Lee, H., Yoo, H., Ko, K., Im, S., & Kim, D. (2022). Machine learning and its applications for plasmonics in biology. *Cell Reports Physical Science*, 3(9), 101042. <https://doi.org/10.1016/j.xcrp.2022.101042>
20. Nasrolahi, M., Farmani, A., Horri, A., & Hatami, H. (2025). Grey wolf optimization algorithm in conjunction with the FDTD method to analyze the nanostructure predicated on a plasmonic demultiplexer. *Plasmonics*. <https://doi.org/10.1007/s11468-025-03016-1>
21. S., N., Muthuswamy, J., Alsalman, O., & Patel, S. K. (2025). Graphene-based machine learning-optimized surface plasmon resonance biosensor design for skin cancer detection. *Plasmonics*. <https://doi.org/10.1007/s11468-024-02734-2>
22. Zhao, X., et al. (2023). Graphene-based tunable dual-band absorbers. *Appl. Phys. Lett.*, 122(10), 101901. <https://doi.org/10.1007/s11082-019-1882-0>
23. Amooosoltani, N., Mehrabi, K., Zarifkar, A., Farmani, A., & Yasrebi, N. (2021). Double-ring resonator plasmonic refractive index sensor utilizing dual-band unidirectional reflectionless propagation effect. *Plasmonics*, 16(4), 1277–1285. <https://doi.org/10.1007/s11468-021-01395-9>
24. Moon, G., Lee, J., Lee, H., Yoo, H., Ko, K., Im, S., & Kim, D. (2022). Machine learning and its applications for plasmonics in biology. *Cell Reports Physical Science*, 3(9), 101042. <https://doi.org/10.1016/j.xcrp.2022.101042>
25. Das, P., & Varshney, G. (2023). Analysis of a Thin Tunable Silicon-Based Metamaterial Absorber for Sensing Applications. *Silicon*, 15(13), 5647–5658. <https://doi.org/10.1007/s12633-023-02388-5>

26. Li, L., Du, F., Zong, X., Cui, L., & Liu, Y. (2022). Plasmonic crystals fabricated by nanosphere lithography for advanced biosensing. *Applied Optics*, 61(23), 6924–6930. <https://doi.org/10.1364/AO.464826>
27. Farmani, A. (2019). Three-dimensional FDTD analysis of a nanostructured plasmonic sensor in the near-infrared range. *Journal of the Optical Society of America B*, 36(2), 401–407. <https://doi.org/10.1364/JOSAB.36.000401>
28. Farmani, A., Mir, A., & Sharifpour, Z. (2018). Broadly tunable and bidirectional terahertz graphene plasmonic switch based on enhanced Goos-Hänchen effect. *Applied Surface Science*, 453, 358–364. <https://doi.org/10.1016/j.apsusc.2018.05.092>
29. Khani, S., Farmani, A., & Mir, A. (2021). Reconfigurable and scalable 2,4-and 6-channel plasmonics demultiplexer utilizing symmetrical rectangular resonators containing silver nano-rod defects with FDTD method. *Scientific Reports*, 11(1), 13628. <https://doi.org/10.1038/s41598-021-93167-y>
30. Xue, J., Zhang, Y., Guang, Z., Hu, J., Zhao, F., Liu, Y., & Shao, L. (2025). MoS₂ surface plasmon resonance based high-resolution THz biosensor using a dual D-shaped channel micro-structured fiber. *Optics & Laser Technology*, 180, 111387. <https://doi.org/10.1016/j.optlastec.2024.111387>
31. Liu, H., Duan, S., Chen, C., Cui, H., Gao, P., Dai, Y., Gao, Z., Wang, X., & Zhou, T. (2024). Graphene-enabled chiral metasurface for terahertz wavefront manipulation and multiplexing holographic imaging. *Optical Materials*, 147, 114654. <https://doi.org/10.1016/j.optmat.2023.114654>
32. Zhao, X., Yuan, C., Zhu, L., & Yao, J. (2016). Graphene-based tunable terahertz plasmon-induced transparency metamaterial. *Nanoscale*, 8(33), 15273–15280. <https://doi.org/10.1039/C5NR07114C>
33. Butt, M. A. (2024). Plasmonic sensors based on a metal-insulator-metal waveguide - what do we know so far? *Sensors*, 24(22), 7158. <https://doi.org/10.3390/s24227158>
34. Kazanskiy, N. L., Khonina, S. N., & Butt, M. A. (2020). Plasmonic sensors based on metal-insulator-metal waveguides for refractive index sensing applications: A brief review. *Physica E: Low-dimensional Systems and Nanostructures*, 117, 113798. <https://doi.org/10.1016/j.physe.2019.113798>
35. Butt, M. A., Kazanskiy, N. L., & Khonina, S. N. (2022). Advances in Waveguide Bragg Grating Structures, Platforms, and Applications: An Up-to-Date Appraisal. *Biosensors*, 12, 497. <https://doi.org/10.3390/bios12070497>
36. Fallahi, V., Kordrostami, Z., & Hosseini, M. (2024). Sensitivity and quality factor improvement of photonic crystal sensors by geometrical optimization of waveguides and micro-ring resonators combination. *Scientific Reports*, 14(1), 2001. <https://doi.org/10.1038/s41598-024-52363-2>
37. Danaie, M., & Kaatuzian, H. (2010). Design of a photonic crystal differential phase comparator for a Mach-Zehnder switch. *Journal of Optics*, 13(1), 015504. <https://doi.org/10.1088/2040-8978/13/1/015504>
38. Zhang, J.; Hong, Q.; Zou, J.; He, Y.; Yuan, X.; Zhu, Z.; Qin, S. Fano-Resonance in Hybrid Metal-Graphene Metamaterial and Its Application as Mid-Infrared Plasmonic Sensor. *Micromachines* 2020, 11, 268. <https://doi.org/10.3390/mi11030268>
39. Mansuri, M., Mir, A., & Farmani, A. (2021). A tunable nonlinear plasmonic multiplexer/demultiplexer device based on nanoscale ring resonators. *Photonic Network Communications*, 42(3), 209–218. <https://doi.org/10.1007/s11107-021-00953-9>
40. Wang, Q., Ouyang, Z., Lin, M., & Zheng, Y. (2021). High-quality graphene-based tunable absorber based on double-side coupled-cavity effect. *Nanomaterials*, 11(11), 2824. <https://doi.org/10.3390/nano11112824>
41. Sadeghzadeh, M., Mohammadi, A., & Jalali, T. (2025). FDTD study of plasmon-exciton coupling for bio-nanosensors. *Results in Chemistry*, 16, 102450. <https://doi.org/10.1016/j.rechem.2025.102450>
42. Butt, M. A., Kazanskiy, N. L., & Khonina, S. N. (2023). A Review on Photonic Sensing Technologies: Status and Outlook. *Biosensors*, 13(5), 568. <https://doi.org/10.3390/bios13050568>
43. Butt, M. A., Kazanskiy, N. L., & Khonina, S. N. (2020). Nanodots decorated asymmetric metal-insulator-metal waveguide resonator structure based on Fano resonances for refractive index sensing application. *Laser Physics*, 30(7), 076204. <https://doi.org/10.1088/1555-6611/ab9090>
44. Huaqing, L., Gao, Y., Zhu, B., Ren, G., & Jian, S. (2015). A T-shaped high resolution plasmonic demultiplexer based on perturbations of two nanoresonators. *Optics Communications*, 334, 164–169. <https://doi.org/10.1016/j.optcom.2014.08.039>

45. Saha, N., Brunetti, G., Kumar, A., & others. (2022). Highly sensitive refractive index sensor based on polymer Bragg grating: A case study on extracellular vesicles detection. *Biosensors*, 12(6), 415. <https://doi.org/10.3390/bios12060415>
46. Yesilkoy, F., et al. (2019). Ultrasensitive hyperspectral imaging and biodetection enabled by dielectric metasurfaces. *Nat. Photonics*, 13(6), 390–396. <https://doi.org/10.1038/s41566-019-0394-6>
47. Wu, Q., Xiao, Y., Zhao, G., & Song, Q. (2024). Evolutionary processes and applications of microfiber resonant Rings: A systematic exploration for sensitivity enhancement. *Optics and Laser Technology*, 174, 110567. <https://doi.org/10.1016/j.optlastec.2024.110567>
48. Taflove, A., & Hagness, S. C. (2005). *Computational electrodynamics: the finite-difference time-domain method*. Artech House.
49. Lyu, J., Huang, L., Chen, L., Zhu, Y., & Zhuang, S. (2024). Review on the terahertz metasensor: from featureless refractive index sensing to molecular identification. *Photonics Research*, 12(2), 194. <https://doi.org/10.1364/prj.508136>
50. Zhang, Z., Yang, J., He, X., Zhang, J., Huang, J., Chen, D., & Han, Y. (2018). Plasmonic refractive index sensor with high figure of merit based on concentric-rings resonator. *Sensors*, 18(1), 116. <https://doi.org/10.3390/s18010116>
51. Bhalla, N., Pan, Y., Yang, Z., & Payam, A. F. (2020). Opportunities and challenges for biosensors and nanoscale analytical tools for pandemics: COVID-19. *ACS Nano*, 14(7), 7783–7807. <https://doi.org/10.1021/acsnano.0c04421>
52. Khani, S., & Hayati, M. (2022). Optical sensing in single-mode filters based on surface plasmon H-shaped cavities. *Optics Communications*, 505, 127534. <https://doi.org/10.1016/j.optcom.2021.127534>
53. Li, Z., Sun, X., Ma, C., Li, J., Li, X., Guan, B.-O., & Chen, K. (2021). Ultra-narrow-band metamaterial perfect absorber based on surface lattice resonance in a WS₂ nanodisk array. *Optics Express*, 29, 27084–27091. <https://doi.org/10.1364/OE.434349>
54. Špačková, B., Wrobel, P., Bocková, M., & Homola, J. (2016). Optical biosensors based on plasmonic nanostructures: A review. *Proceedings of the IEEE*, 104(12), 2380–2408. <https://doi.org/10.1109/JPROC.2016.2624340>
55. Khani, S., Danaie, M., & Rezaei, P. (2020). Realization of a plasmonic optical switch using improved nano-disk resonators with Kerr-type nonlinearity: A theoretical and numerical study on challenges and solutions. *Optics Communications*, 477, 126359. <https://doi.org/10.1016/j.optcom.2020.126359>
56. Danaie, M., & Shahzadi, A. (2019). Design of a high-resolution metal-insulator-metal plasmonic refractive index sensor based on a ring-shaped Si resonator. *Plasmonics*, 14. <https://doi.org/10.1007/s11468-019-00926-9>
57. Guo, R., Gao, H., Liu, T., & Cheng, Z. (2022). Ultra-thin mid-infrared silicon grating coupler. *Optics Letters*, 47, 1226–1229. <https://doi.org/10.1364/OL.449140>
58. Alipour, A., Mir, A., & Farmani, A. (2020). Analytical modeling and design of a graphene metasurface sensor for thermo-optical detection of terahertz plasmons. *IEEE Sensors Journal*. <https://doi.org/10.1109/JSEN.2020.303557710>
59. Farmani, A., Mir, A., & Sharifpour, Z. (2018). Broadly tunable and bidirectional terahertz graphene plasmonic switch based on enhanced Goos-Hänchen effect. *Applied Surface Science*, 453, 358–364. <https://doi.org/10.1016/j.apsusc.2018.05.092>
60. Lu, Y., Rhee, J., Jang, W., & Lee, Y. (2010). Active manipulation of plasmonic electromagnetically-induced transparency based on magnetic plasmon resonance. *Optics Express*, 18, 20912–20917. <https://doi.org/10.1364/OE.18.020912>
61. Farmani, A., Miri, M., & Sheikhi, M. H. (2017). Analytical modeling of highly tunable giant lateral shift in total reflection of light beams from a graphene containing structure. *Optics Communications*, 391, 68–76. <https://doi.org/10.1016/j.optcom.2017.01.018>
62. Arellano Vidal, C. L., & Govan, J. E. (2024). Machine learning techniques for improving nanosensors in agroenvironmental applications. *Agronomy*, 14(2), 341. <https://doi.org/10.3390/agronomy14020341>
63. Divya, J., Selvendran, S., Raja, A. S., & Sivasubramanian, A. (2022). Surface plasmon based plasmonic sensors: A review on their past, present and future. *Biosensors and Bioelectronics*: X, 11, 100175. <https://doi.org/10.1016/j.biosx.2022.100175>
64. Sun, X., Mojahedi, M., & Aitchison, J. S. (2016). Hybrid plasmonic waveguide-based ultra-low insertion loss transverse electric-pass polarizer. *Optics Letters*, 41(17), 4020–4023. <https://doi.org/10.1364/OL.41.004020>

65. Wang, Y., et al. (2021). Wearable plasmonic-metasurface sensor for noninvasive and universal molecular fingerprint detection on biointerfaces. *Sci. Adv.*, 7(4), eabe4553. <https://doi.org/10.1126/sciadv.abe4553>
66. Dmitriev, P. A., Lassalle, E., Ding, L., Pan, Z., Neo, D. C. J., Valuckas, V., Paniagua-Dominguez, R., Yang, J. K. W., Demir, H. V., & Kuznetsov, A. I. (2023). Hybrid dielectric-plasmonic nanoantenna with multiresonances for subwavelength photon sources. *ACS Photonics*, 10(3), 582-594. <https://doi.org/10.1021/acsp Photonics.2c01332>
67. Wang, S., Zhu, Y., Luo, S., Zhu, E., & Chen, S. (2021). Compact hybrid plasmonic slot waveguide sensor with a giant enhancement factor for surface-enhanced Raman scattering application. *Optics Express*, 29, 24765-24778. <https://doi.org/10.1364/OE.431274>
68. Nasrolahi, M., Farmani, A., Horri, A., & Hatami, H. (2024). FDTD analysis of a high-sensitivity refractive index sensing based on Fano resonances in a plasmonic planar split-ring resonators. *Journal of Optical and Photonic Nanostructures*, 9(3), 91-115. <https://doi.org/10.30495/jopn.2024.33499.1321>
69. Farmani, A., & Mir, A. (2019). Graphene sensor based on surface plasmon resonance for optical scanning. *IEEE Photonics Technology Letters*, 31(8), 643-646. <https://doi.org/10.1109/LPT.2019.2904618>
70. Butt, M. A., Khonina, S. N., & Kazanskiy, N. L. (2021). Recent advances in photonic crystal optical devices: A review. *Optics & Laser Technology*, 142, 107265. <https://doi.org/10.1016/j.optlastec.2021.107265>
71. Farmani, A., Miri, M., & Sheikhi, M. H. (2017). Analytical modeling of highly tunable giant lateral shift in total reflection of light beams from a graphene containing structure. *Optics Communications*, 391, 68-76. <https://doi.org/10.1016/j.optcom.2017.01.018>
72. Farmani, A., Mir, A., & Sharifpour, Z. (2018). Broadly tunable and bidirectional terahertz graphene plasmonic switch based on enhanced Goos-Hänchen effect. *Applied Surface Science*, 453, 358-364. <https://doi.org/10.1016/j.apsusc.2018.05.092>
73. Butt, M. A., Khonina, S. N., & Kazanskiy, N. L. (2021). Recent advances in photonic crystal optical devices: A review. *Optics & Laser Technology*, 142, 107265. <https://doi.org/10.1016/j.optlastec.2021.107265>